

# Fabrication of novel nanocomposite nanofibrous matrices retaining high concentration of microbial cells for heavy crude oil biodegradation

A. Partovinia<sup>1\*</sup>, M. Koosha<sup>2</sup>

<sup>1</sup>Bioprocess Engineering Laboratory, Faculty of New Technologies Engineering, Zirab Campus, Shahid Beheshti University, Tehran, Iran

<sup>2</sup>Nano-structured Fibers Division, Faculty of New Technologies Engineering, Zirab Campus, Shahid Beheshti University, Tehran, Iran

Received 26 October 2018; accepted in revised form 5 January 2019

**Abstract.** Microbial cells immobilized in porous carriers as an effective technique has been recently studied and applied in various applications including wastewater treatment. High mechanical stability and large specific surface area are the key advantages of an ideal porous carrier. Immobilization of microbial cells in novel nanocomposite nanofibrous webs (NC-NFWs) for use in bioremediation of heavy crude oil as sole carbon and energy sources in aqueous phase was the main focus of this study. Polyvinyl alcohol (PVA) and alginate (ALG) were selected as the polymer matrices for the electrospinning of nanofibrous webs (NFWs). In this study, preparation and application of PVA/ALG webs that were reinforced by halloysite nanotubes (HNTs) followed by cross-linking with glyoxal (GO) are described for the first time. The synthesized NFWs were characterized using Fourier transform infrared spectroscopy (FTIR), X-ray diffractometry (XRD), scanning electron microscopy (SEM) and tensile tests. Results showed that NC-NFWs have a great potential for bioremediation of crude oil, and removal performances were higher in immobilized systems (85 and 64%) compared to freely suspended cell system (48%) after 14 days. Also, maximal bacterial growth in culture containing 500 ppm crude oil was achieved by PVA/ALG/GO/HNT7.5% which was almost 1.4 and 2.4 times higher than PVA/ALG/GO/HNT5% and free cell system at same inoculum concentration, respectively.

**Keywords:** polymer composites, electrospinning, halloysite nanotubes, nanocomposites, reinforcements

## 1. Introduction

There are different types of pollutants in industrial wastewater effluents. Diverse technologies including physical, chemical and biotechnological techniques have been proposed and applied to remove pollutants from wastewater streams [1, 2]. Due to relatively the high cost and low efficiency of physicochemical methods in pollutants removal, bioremediation as a promising technique has been developed in wastewater treatments in recent years [3, 4]. Immobilization technique, confinement of biocatalysts such as enzymes and whole cells inside or on the carrier or support

material is often considered to be a more practical method compared to other biotechnological methods due to possible reutilization of microorganisms, easier separation, and stability against tensions of prohibitive materials and toxic metabolites over long time periods [5, 6]. The efficiency of immobilization technique is dependent on appropriate amount of microbial cells and potential of microbial cell attachment to the carrier [1, 7–14]. Cell attachment to a surface is a simple immobilization technique in which cells are adsorbed to a solid support [5]. Microbial cells also can diffuse into the carrier and immobilize

\*Corresponding author, e-mail: [a\\_partovi@sbu.ac.ir](mailto:a_partovi@sbu.ac.ir)  
© BME-PT

by different interactions (i.e. hydrogen bonding, van der Waals attraction, gravitational forces, surface electrostatic charges, hydrophilic/hydrophobic interactions and production of microbial exopolymers) which have been introduced in our review [15]. Hydrophobic–hydrophilic nature of microbial cells is one of the important factors that can increase the adhesion tendency of cells. More hydrophobic microbial cells adhere more strongly to hydrophobic supports and also hydrophilic microbial cells strongly adhere to hydrophilic surfaces [16]. Measurement of water contact angle and interfacial free energy of *Bacillus licheniformis* have indicated that the cell surface is hydrophilic. Therefore it can be concluded that it is more efficient to adhere to hydrophilic matrices [17].

Microbial cell and material surface interactions, adhesion properties of surface and increment of surface area to volume ratio are crucial factors for selection of carriers in biological applications [11, 18–20]. Until now, different hybrid matrices prepared by both inorganic (e.g. bentonite, silica, glass, metals, etc.) and organic materials (polysaccharides, cellulose, agar, starch, proteins, polystyrene, polyacrylamide, polyurethane, etc.) have been successfully applied for the cell immobilization. As we have reported previously, the combination of sodium alginate (ALG), a natural polymer, and poly(vinyl alcohol) (PVA), a synthetic polymer, has recently drawn attention due to their low-cost, nontoxicity, and biological compatibility as well as their reusability and long-term stability for environmental applications. Alginate and PVA also have hydrophilic nature that are also particularly useful for immobilization of microbial cells with hydrophilic surfaces. Moreover, to allow the transfer of hydrophobic compounds, their matrix should be porous enough [15].

In recent years, spherical hybrid hydrogel beads of PVA-ALG have been known as a promising matrix for cell immobilization systems. However, researchers have observed that PVA/ALG beads were dissolved after a short time. On the other hand, cell damage in the boric acid solution and agglomeration of PVA beads are the other important limitations of this matrix [21, 22]. Although solubility problem have been resolved by addition of sodium sulfate to PVA/ALG beads [23, 24] but its specific surface areas still remains challenging. The large surface to volume ratio of carriers enhances the cell attachment, mass transfer and thereafter bioprocess capacity [5, 18, 25].

Electrospinning is one of the best techniques for the fabrication of nanofiber webs (NFWs) with high surface area and porosity which are made from polymer-based fibers with diameters lower than 100 nm [26]. However, biodegradation of pollutants in water systems using NFWs have been previously investigated by several researchers [27–32] but to the best of our knowledge, no report exists in applying NFW of PVA/ALG for bioprocess engineering.

Electrospinning of living bacteria has been restricted to water-soluble polymers. On the other hand, easily dissolution of PVA/ALG webs in aqueous solutions and its weak mechanical strength cause limitations for enzyme and cell immobilization [33, 34]. Therefore, most of the previous studies in cell immobilization field are focusing on different cross-linking agents such as boric acid, calcium chloride, and glutaraldehyde to improve physical properties of the carriers and overcome these limitations [35–37]. Glyoxal (GO) is also recognized as a potent crosslinking agent in polymer chemistry [38]. Besides, halloysite nanotubes (HNTs) have been used to prepare reinforced organic-inorganic nanocomposites. Halloysite clay is an aluminosilicate nanotube with positively charged inner lumen and the negatively charged outer surface which are made of aluminum hydroxide and silicon dioxide respectively [39]. Also, HNT has been introduced as a feasible support for encapsulation of drugs and enzymes [40]. In contrast to the carbon nanotubes which are toxic nanomaterials, HNT is a biocompatible and nontoxic natural nanotube and its loading procedure is also simple [41]. Immobilized laccase enzyme on the surface of HNT exhibited a rapid degradation rate and high degradation efficiency for removal of phenol compounds [42].

Hence, the main object of this work is to fabricate a novel PVA/alginate/HNT NFW with high mechanical strength and high surface area to weight ratio. The other goal of this survey is to examine the ability of cell attachment to the novel matrices. These matrices can be prepared by both organic (PVA/ALG) and inorganic (HNT) carriers for biological applications in the aqueous phase experiments. Therefore, the carrier was prepared with three different compositions to find the best formulation for industrial applications. For this reason, we have fabricated electrospun nanofiber mats of PVA/ALG as a potent hybrid matrix for microbial cell immobilization, with large surface to volume ratio to enhance cell attachment capacity. GO as a crosslinker and HNT as a

potential candidate in the class of nanofillers were added to PVA/ALG matrix to reinforce the structure of hybrid and improve the stability in aqueous environment for successive reuse of immobilized biocatalyst.

## 2. Materials and methods

### 2.1. Materials

PVA (molecular weight about 200 000 g/mol, degree of hydrolysis >0.85) was purchased from Merck. ALG for cell immobilization was purchased from Sigma. Double distilled water (DDW) was used as solvent for solution preparation.  $\text{CaCl}_2$ , glyoxal (GO) (40% in water), HCl (37%), and dichloromethane were also purchased from Merck. HNT was supplied by NaturalNano Corporation (USA). GO was mixed with HCl at 1 vol% and used as crosslinking agent (GO/HCl). Iranian heavy crude oil with API and specific gravity of 29 and 0.8814 kg/l, respectively, have been used as the sole carbon and energy sources for bioremediation studies.

### 2.2. Microorganism and culture media

An isolated *Bacillus licheniformis* bacterium as a known biosurfactant producer was used in the study. It was grown in nutrient broth (NB, lot number 12794217, ibresco, Iran) and incubated at 30 °C and 150 rpm until the mid-logarithmic phase. The culture was then centrifuged at 2000 rpm for 10 min and cells were re-suspended in NaCl solution (8.5 g/l) to reach an optical density (600 nm) of about 1 to obtain a uniform bacterial population for inoculation.

The mineral salt medium (MSM) for cultivation consisted of (in g/l):  $\text{NH}_4\text{Cl}$ , 1;  $\text{KH}_2\text{PO}_4$ , 1.09;  $\text{Na}_2\text{HPO}_4$ , 2.14;  $\text{MgSO}_4 \cdot 7\text{H}_2\text{O}$ , 0.2;  $\text{FeSO}_4 \cdot 7\text{H}_2\text{O}$ , 0.003;  $\text{CaCl}_2$ , 0.01;  $\text{MnCl}_2 \cdot 4\text{H}_2\text{O}$ , 0.0018;  $\text{Co}(\text{NO}_3)_2 \cdot 6\text{H}_2\text{O}$ , 0.0013;  $\text{ZnSO}_4 \cdot 7\text{H}_2\text{O}$ , 0.00004;  $\text{H}_2\text{MoO}_4$ , 0.00002 and  $\text{CuSO}_4 \cdot 5\text{H}_2\text{O}$ , 0.00001 in distilled water. The pH of MSM was adjusted to 7. All mineral salts were purchased from Merck.

### 2.3. Solution preparation

PVA was dissolved in DDW with a concentration of 12% by vigorous stirring at 80 °C. A 2% ALG solution was prepared by magnetic stirring at room temperature. Both solutions were allowed to stir at room temperature overnight and then mixed with a volume ratio of 70:30 (PVA/ALG). A volume of GO/HCl solution equal to 10 vol% of PVA/ALG solution was

added to crosslink the polymers. The resulting nanofibers were named as PVA/ALG/GO.

To prepare NC-NFWs, HNT was dispersed in water with a concentration of 1% at 70 °C by magnetic stirring for 3 hr. Two other solutions were prepared by addition of appropriate amounts of HNT dispersion to the PVA/ALG solution so that the final concentration of HNT based on the polymers present in the solutions were 5 and 7.5%. Finally the GO was added at 10 vol% of the total solution to crosslink the polymers. The resulting nanofibers were named as PVA/ALG/GO/HNT5% and PVA/ALG/GO/HNT7.5%.

### 2.4. Electrospinning

The solutions were electrospun with an electrospinning apparatus (Fanavaran Nanomeghyas Company, Tehran, Iran) at a voltage of 15 kV, tip to collector distance of 6 cm and flow rate of 0.2 ml/h using a G19 syringe needle (inner diameter = 0.69 mm).

### 2.5. Characterization

#### 2.5.1. Scanning electron microscopy (SEM)/energy dispersive X-ray scattering (EDX)

The morphology of the electrospun nanofibers was observed using a Hitachi SEM (SU3500, Japan) device. The samples were sputter coated with Au before the test. In order to map the distribution of HNTs into the nanofiber matrix, back scattered electrons were detected by EDX analyzer and the presence of Si atoms was identified in the composition of NC-NFWs. The average size of nanofibers was measured using ImageJ software. At least 20 fibers were selected and their sizes were measured. Also, the average pore size of the nanofibers was obtained by measuring the diameter of the free spaces between nanofibers.

#### 2.5.2. X-ray diffraction (XRD)

XRD patterns of the electrospun nanofibers as well as the raw materials were recorded from  $2\theta = 2-60^\circ$  by a Stoe powder diffraction system (STOE & Cie, Germany). The diffraction source was Cu K- $\alpha$  with a wavelength of 1.54 Å.

#### 2.5.3. FTIR

FTIR spectra of the nanofibers were obtained by ATR-FTIR (Thermo Nicolet, Nexus 470, USA).

#### 2.5.4. Mechanical properties

To measure the mechanical properties of the nanofibers, each sample was cut into 4 cm×5 mm with a rectangular shape. The thickness was recorded for each sample before the test. A universal tensile testing machine (Instron 5566, USA) was used with a load cell of 50 N. Each sample was placed between the grips with a gauge length of 3 cm and extended with a rate of 10 mm/min up to break. Three replicates were tested for each sample and the average results were reported.

#### 2.5.5. Swelling ratio measurement

The swelling ratio measurement was carried out in distilled water. The weight swelling ratio, defined as the difference between the weight of sample after swelling and the dry weight divided by the weight of the dry sample, was determined as a function of time. For each matrix, the average of three measurements of swelling ratio was reported.

#### 2.6. Microbial cell attachment on NC-NFWs

In this study, cell immobilization was performed according to Oh *et al.* [43] (2000) by freeze drying after absorption of cells in the preformed matrices. For freeze drying, the prepared NC-NFWs were soaked in a bacterial cells suspension to make a cell density of  $1.4 \cdot 10^8$  CFU per 5 mg of matrices, and transferred to freezer for 24 h and then lyophilized by a freeze drier (model SEPEC 01, Zist Faryand Tajhiz, Tabriz, Iran) for 24 h to remove water. Thereafter, matrices carefully washed with distilled water to remove unattached bacteria and SEM test of the webs was also performed after dehydration. For biodegradation study, the produced matrices transferred to flasks supplied with MSM containing crude oil. Physicochemical stability of prepared nanocomposite webs were examined by shaking the matrices in various salt solutions (KCl, NaCl, and  $\text{NaHCO}_3$  1N) for 30 days at 30 °C and 150 rpm [12, 44].

#### 2.7. Heavy crude oil biodegradation experiments

Biodegradation studies were carried out in 100 ml flasks containing 25 ml MSM and 500 ppm heavy crude oil. 5 mg of PVA/ALG/GO webs (NC-NFWs with HNT 5% and 7.5%) containing about  $1.4 \cdot 10^8$  CFU were added into flasks and incubated at 30 °C for 14 days at 150 rpm. Biodegradation was compared with freely suspended cell system in which

equivalent amount of cells in the culture has been used. All experiments were performed in duplicate. Biodegradation of crude oil was separately investigated in free cell (FC) and immobilized cell (IC) systems by measuring bacterial growth in aqueous phase using optical density measurement with spectrophotometer (Unico 280 UV/VIS, U.K.). To extract residual crude oil from cultures, 25 ml solvent (dichloromethane) was added to each flask containing 25 ml mineral salt medium and flasks were vigorously mixed and then placed on a rotary shaker at 200 rpm for 3 h. The mixture of aqueous phase and solvent was separated by decantation after standing for 30 min. The crude oil content extracted with dichloromethane was determined gravimetrically in an analytical electronic balance (Mettler Toledo JB1603-C/FACT, Switzerland) as the amount of total petroleum hydrocarbons [45].

Control experiments consist of MSM and NC-NFWs without inocula were carried out for assessment of non-biological degradation. Additionally, for examination of the microbial cells detachment from the nanocomposite matrices and the release of bacteria from carrier to the solution, the bacteria-immobilized nanofibrous webs were transferred to the flask containing MSM without crude oil and the optical density of culture was measured at 600 nm. Moreover, another experiment was conducted to evaluate the possible degradation of polymer matrix, in the presence of free bacterial cells without crude oil.

### 3. Results and discussion

#### 3.1. Morphology

Morphology of the nanofibers as well as nanocomposite nanofibers produced in this research is presented in Figure 1. Uniform bead-free nanofibers were observed for uncrosslinked PVA/ALG sample (Figure 1a) in accordance with the literature data [46]. For PVA/ALG/GO sample which is crosslinked by GO, the morphology has been significantly changed. It is seen that the nanofibers were merged into each other, flattening the nanofibrous mat (Figure 1b). Formation of this morphology may be related to the crosslinking effect of GO producing a dense polymeric network by formation of chemical bonds which increase the viscosity and merge the nanofibers into each other. In case of nanocomposite nanofibers, a more uniform morphology was seen (Figure 1c, 1d), however, the shape and size of the nanofibers was altered after addition of HNT to the



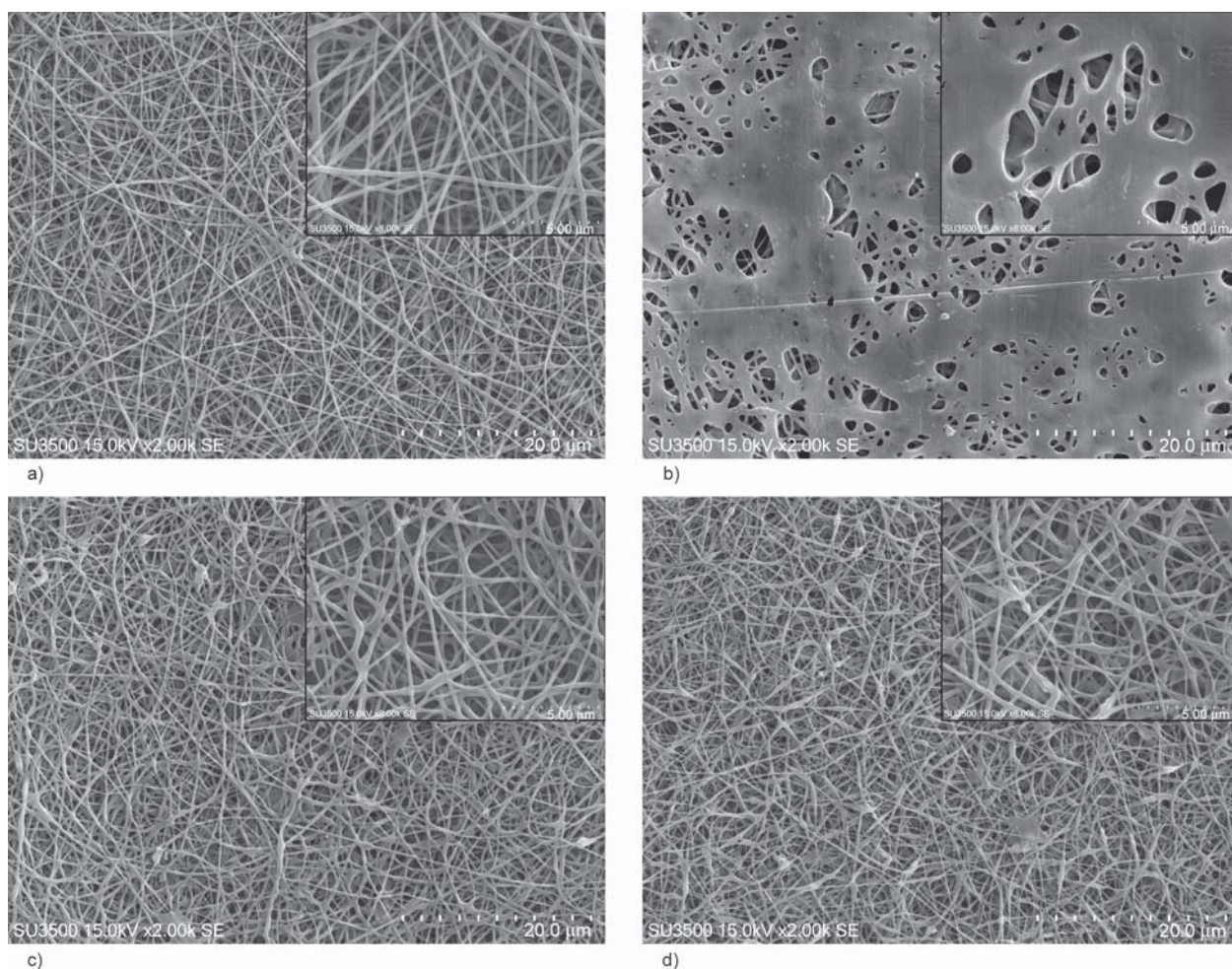


**Figure 1.** SEM images of the electrospun PVA/ALG (a), PVA/ALG/GO (b), PVA/ALG/GO/HNT5% (c) and PVA/ALG/GO/HNT7.5% (d) at two different magnifications.

PVA/ALG solutions. By increasing the HNT content to 7.5%, the shape of the nanocomposite nanofibers was nearly a spindle-like morphology (Figure 1d). This observation is common when nanoclays are present inside the nanofibers. The nanocomposite nanofibers reinforced by HNT had a fewer number of merged nanofibers and flattened areas. It is well known that in the electrospinning process, the conductivity and concentration of polymer solution plays a very important role in fiber formation and morphology of the resulting fibers [47]. In this work, the solution intercalation method was used for incorporation of HNTs into polymer solutions. HNT was dispersed in water and a predetermined volume of the dispersion was added to the polymer solution and electrospun. When a dispersion of HNT is added to PVA/ALG solution, an excess amount of solvent (water) enters to the polymer solution which reduces the total concentration of polymer chains and reduces the viscosity. Addition of HNT into the polymer solution increases the conductivity and results

in a higher charge density on the surface of solution jet which favors the fiber formation with a more uniform morphology and fewer beads. Reduction of the viscosity of polymer solutions by HNT addition also enhances the morphology of nanocomposite nanofibers. Similar results has been reported in our previous work on electrospun chitosan/PVA/nanoclay [48] as well as polycaprolactone/nanoclay [49], polymethyl methacrylate/nanoclay [50] and polyurethane/nanoclay [51] nanocomposite nanofibers. The average size of the nanofibers was also reduced by addition of HNT (Table 1). As mentioned, the addition of HNT to the PVA/ALG solutions reduces the total polymer concentration and lowers the viscosity of the solutions. Reduction of the solution viscosity produces smaller nanofibers in the electrospinning process. On the other hand, it can be seen (Figure 1c, 1d) that the micro-pores in NC-NFWs are completely interconnected, implying that the web structure has an excellent potential for cell attachment and hence are suitable for transfer of substrate and nutrients. Li *et al.*

**Table 1.** Size distribution of nanofibers for PVA/ALG, PVA/ALG/GO, PVA/ALG/GO/HNT5% and PVA/ALG/GO/HNT7.5%.

	PVA/ALG	PVA/ALG/GO	PVA/ALG/GO/HNT5%	PVA/ALG/GO/HNT7.5%
Mean of fiber diameter [nm]	217	428	195	143
Standard deviation	48	84	55	40
Min	112	328	100	78
Max	351	639	399	243

[52] (2005) have reported that substrate and oxygen could diffuse easily into and from the ALG microbeads with pore size of about 2  $\mu\text{m}$ .

In this study, the average pore size of PVA/ALG/GO/HNT5% is comparatively larger than the PVA/ALG/GO/HNT7.5%. It is noteworthy that matrices with small pore size are suitable for usage in bioreactor due to their minimized cell release and avoidance of cell washout from the bioreactor. However, matrices with high porosity are the best choice for field applications [53]. Therefore, we conclude that addition of HNT affects the pore size, as a criterion of cell protection and prevention of cell release, as well as mass transfer.

When HNT nanotubes are added to polymer solutions, it is important to prove its presence in the nanofiber mat. SEM/EDX results give us the opportunity to map the distribution of HNT within the PVA/ALG matrix due to their different chemical structure compared with PVA and ALG. SEM images, EDX mapping and spectra for PVA/ALG/GO/HNT5% (Figure 2a–2c) and PVA/ALG/GO/HNT7.5% (Figure 2d–2f) demonstrate the presence and distribution of HNT in the NC-NFWs. In both HNT contents (5 and 7.5%) a good dispersion was observed with few aggregates. This is a result of the solution intercalation method used for dispersion of HNT into polymer matrix. Also, the high voltage electric field of the electrospinning process applied to the solution draws the jet with a strong electrical force which breaks the aggregates of nanotubes present in the solution.

### 3.2. XRD analysis

XRD patterns of pristine materials used for preparation of nanocomposite nanofibers show the characteristic peaks related to PVA, ALG and HNT (Figure 3a). The spectrum observed for PVA showed major peaks at 19.8 and 22.16 related to its crystalline structure [54]. ALG showed two peaks at 13.6 and 21.6 [55], however, the peaks were broad indicating that ALG has a low crystallinity. HNT main peaks were appeared at 11.9, 19.8 and 24.2. The basal spacing

of the pristine HNT calculated from Bragg's law is  $\sim 7.4 \text{ \AA}$  ( $2\theta = 11.9^\circ$ ) [56].

In case of PVA/ALG nanofibers (Figure 3b), one peak was observed at  $2\theta = 19^\circ$  and all of the other characteristic peaks of pure PVA and ALG were absent. This result reveals that the crystalline structure of PVA was altered by blending with ALG and electrospinning. Though, PVA/ALG nanofibers show an amorphous morphology with a low crystallinity. Similar result has been observed in the electrospinning of PVA/ALG/ZnO nanofibers [57]. Two reasons can be mentioned for the amorphous behavior of PVA/ALG nanofibers. One is the low compatibility between PVA and ALG chains. PVA chains have a random coil configuration while ALG is a polysaccharide with rod-like macromolecules. Although, PVA and ALG solutions are miscible due to favorable hydrogen bonding interactions however, the difference in their chain structure results in incompatibility in the molecular scale. Thus, blending ALG with PVA solution prevents the crystal formation of PVA chains due to their incompatibility. The second reason is that in electrospinning process, the solvent rapidly evaporates and polymer chains orient into fibrous structures. Crystallization of the nanofibers is thermodynamically favorable in the electrospinning process but rapid evaporation of solvent hinders it kinetically. The chains do not have enough time to form crystals resulting in amorphous nanofibers.

The intensity of the peak for PVA/ALG/GO was slightly increased by addition of GO due to the cross-linking reactions occurred between PVA and ALG chains. For PVA/ALG/GO/HNT5% and PVA/ALG/GO/HNT7.5% the intensity of the crystalline peak was decreased and the peaks are broader indicating the above mentioned amorphous morphology. Also, two peaks were observed due to intercalation of HNT in the PVA/ALG matrix (10.9 and 5.6 for PVA/ALG/GO/HNT5% and 11.5 and 7.1 for PVA/ALG/GO/HNT7.5%). It seems that nanotubes had a better dispersion in the sample PVA/ALG/GO/HNT5% because the HNT peaks were shifted to lower  $2\theta$  values. The



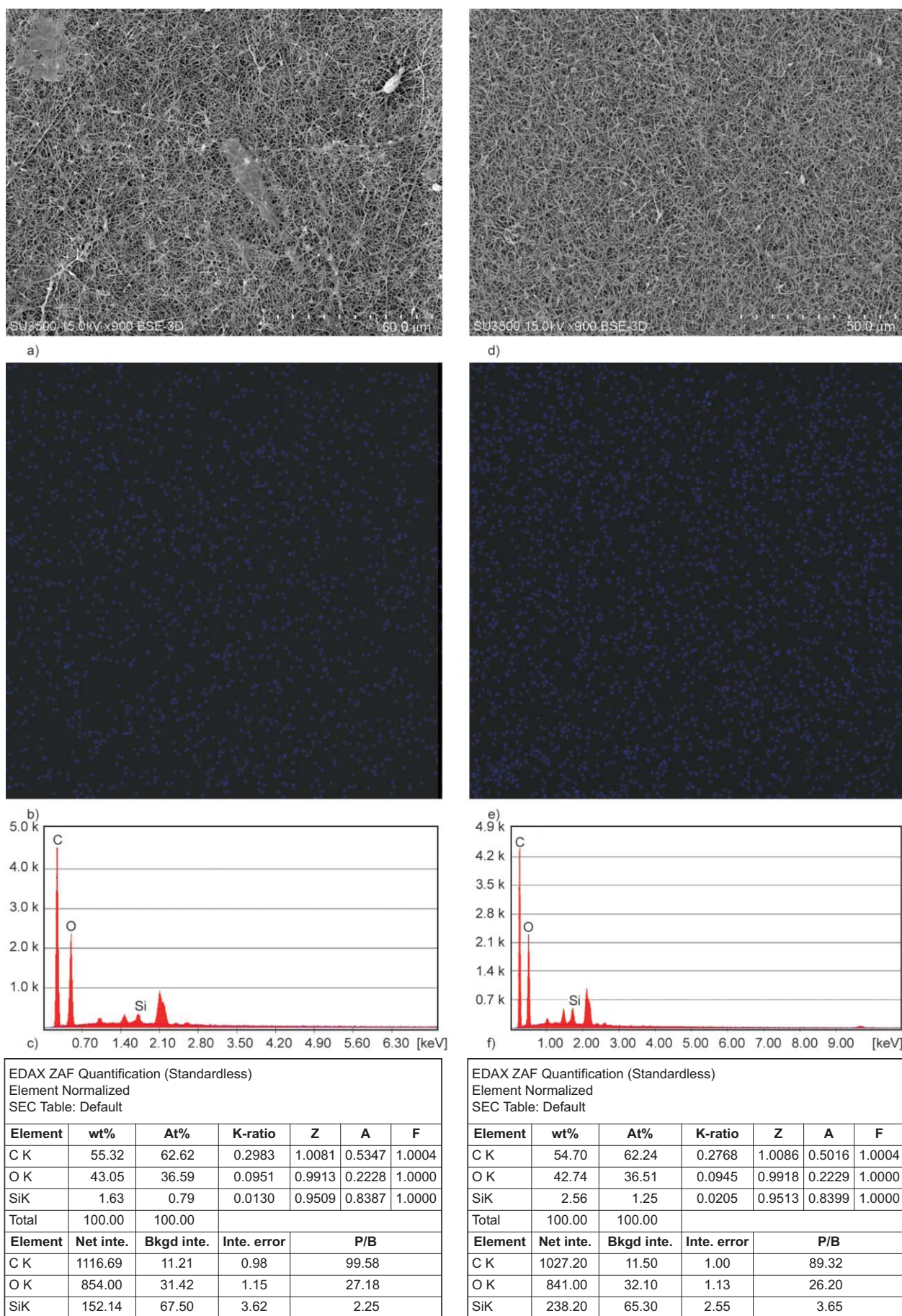


**Figure 2.** SEM/EDX mapping, spectra and analysis for PVA/ALG/GO/HNT5% (a–c) and PVA/ALG/GO/HNT7.5% (d–f).

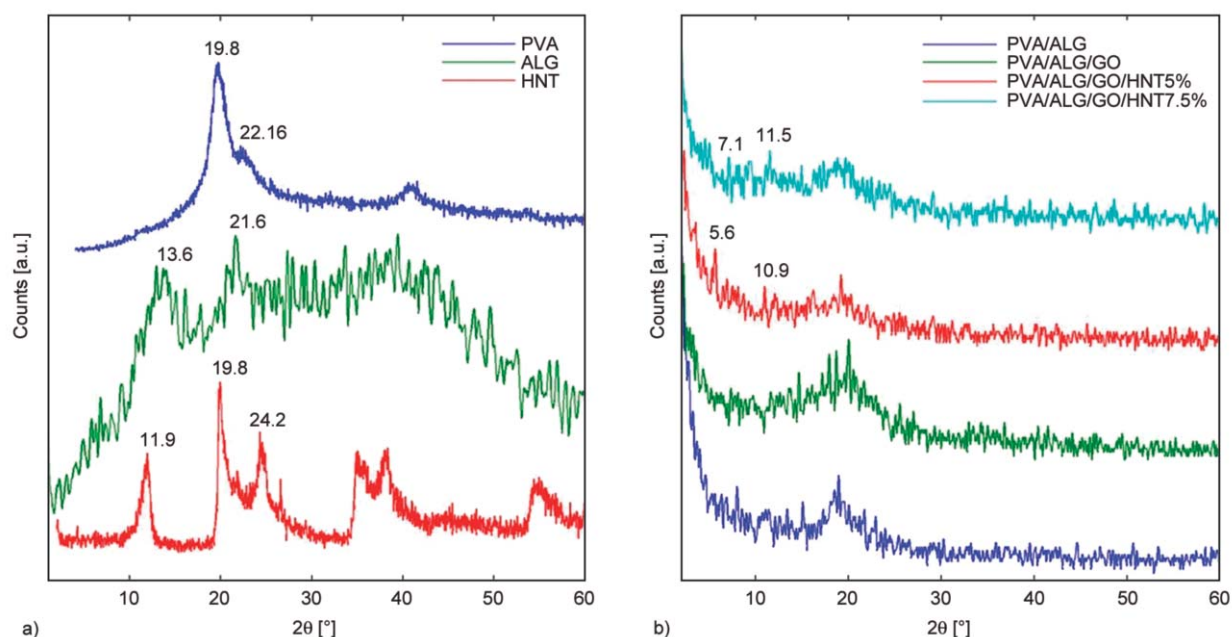


**Figure 3.** XRD data of pristine materials (a) and electrospun nanocomposite nanofibers (b).

reason for this result can be related to the lower amount of HNT in the polymer solution because when the concentration is low, the aggregates of HNT can break down more during the electrospinning process.

### 3.3. Chemical analysis

FTIR spectroscopy can provide valuable data about the chemical structure and reactions occurred between polymers and the crosslinker as well as interactions between polymer chains. In the spectrum obtained for the pristine materials used in this study, relevant peaks can be observed for each material (Figure 4a). For PVA, main peaks at wavenumbers of 3440, 2940, 1740 and 850  $\text{cm}^{-1}$  are respectively related to OH stretching vibrations, antisymmetric  $\text{CH}_2$  stretching, C=O vibrations and C–H bond rocking [54]. ALG bands at 3253, 1593–1408, 1082–1024  $\text{cm}^{-1}$

are assignable to OH stretching vibrations, antisymmetric and symmetric  $\text{COO}^-$  stretching vibrations and antisymmetric C–O–C vibrations and OH bending vibrations, respectively [58, 59]. Glyoxal showed peaks at 3370, 1640, 1420 and 1060  $\text{cm}^{-1}$  relating to OH stretching vibrations, aldehyde C=O vibrations,  $\text{CH}_2$  wagging and C–O stretching vibrations, respectively [60]. HNT major peaks were appeared at 3700, 3620, 1640, 1030, 912, 536 and 468  $\text{cm}^{-1}$  which can be related to Al–OH vibrations, stretching of inner OH groups, interlayer water vibrations, in-plane Si–O stretching, Al–O vibrations, OH deformation of inner hydroxyl groups, Al–O–Si vibrations, Si–O–Si vibrations, respectively [61, 62].

In case of PVA/ALG nanofibers (Figure 4b), OH stretching vibrations were appeared at 3288  $\text{cm}^{-1}$ . This wavenumber lies between the stretching vibrations of PVA (3440  $\text{cm}^{-1}$ ) and ALG (3253  $\text{cm}^{-1}$ ) which

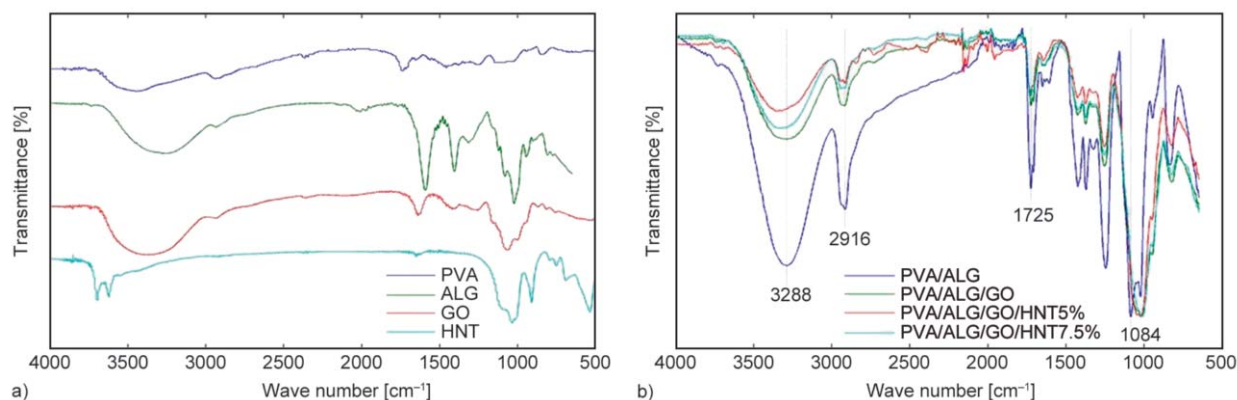


**Figure 4.** FTIR spectra of pristine materials (a) and electrospun nanofiber mats (b).



indicates possible hydrogen bonding interactions between OH groups of PVA and ALG. By addition of GO to the PVA/ALG solutions, the intensity of the band at  $3288\text{ cm}^{-1}$  was highly reduced indicating that concentration of OH groups was reduced. This result proves that chemical reactions were occurred between GO and OH groups of PVA and ALG chains as reported in the literature [38]. GO is a reactive dialdehyde which can react with hydroxyl groups forming ether bonds between the polymer chains. The band observed for PVA/ALG nanofibers at  $1084\text{ cm}^{-1}$  which was related to C–O–C stretching vibrations is shifted to lower wavenumbers for the crosslinked samples. It means that higher energy is required for the vibrations of C–O–C bonds after addition of GO. This result also can be another evidence for the occurrence of crosslinking reactions between GO and the polymer chains because crosslinking by GO increases the number of C–O–C bonds.

For the samples reinforced with HNT, the observed peaks are similar to that of PVA/ALG/GO samples indicating that crosslinking reaction was also occurred for these samples. Vibrations of hydroxyl group were appeared at the wavenumbers of  $3350$  and  $3335\text{ cm}^{-1}$  for PVA/ALG/GO/HNT5% and PVA/ALG/GO/HNT7.5%, respectively. They have shifted to higher values compared to the sample PVA/ALG/GO ( $3288\text{ cm}^{-1}$ ) due to the incorporation of HNT ( $3620$  and  $3690\text{ cm}^{-1}$ ). HNT shows two peaks in the range  $3000\text{--}4000\text{ cm}^{-1}$  but we only observed one peak for the HNT-reinforced samples, which indicates that favorable interactions were occurred between hydroxyl groups of PVA and ALG and OH groups present on the surface of HNT. The intensity of OH group for PVA/ALG/GO/HNT5% was lower compared to PVA/ALG/GO/HNT7.5%. This result, in accordance with our SEM/EDX and XRD data, shows that HNTs were properly dispersed in the matrix of PVA/ALG when their concentration was 5%. The better dispersion of HNTs provides more surface area available for hydrogen bonding interactions. Thus, the intensity of OH groups was reduced due to better dispersion.

### 3.4. Tensile strength

Mechanical properties of nanofibers play an important role for using them in many applications. In this work, the addition of GO to PVA/ALG resulted in a slight reduction of tensile strength however, it was statistically not significant ( $p\text{-value} > 0.1$ ) (Figure 5a)

while when HNT was added, the tensile strength was increased, effectively ( $p\text{-value} < 0.0005$ ). This result shows the reinforcing effect of HNT and enhancing the mechanical properties of PVA/ALG nanofibers. It also shows that the addition of GO only cannot increase the tensile strength while presence of GO and HNT simultaneously can improve the tensile strength of PVA/ALG nanofibers. Although HNT was used in many works to prepare nanocomposite films or gels [56, 63–67], however, to the best of our knowledge, this is the first study on reinforcing PVA/ALG nanofibers with HNT nanoclay.

The elastic modulus and maximum strain (at tensile strength) of the samples are presented in Figure 5b, 5c. The elastic modulus was significantly increased for PVA/ALG/GO and PVA/ALG/GO/HNT5% comparing to PVA/ALG ( $p\text{-value} < 0.01$ ) but decreased for PVA/ALG/GO/HNT7.5%. The increment in elastic modulus for PVA/ALG GO is due to the crosslinking reactions occurred between PVA and ALG chains leading to formation of polymeric network and increasing the modulus. Addition of HNT usually increases the elastic modulus in most polymer/clay nanocomposites. In our work, the elastic modulus was increased for PVA/ALG/GO/HNT5% due to the effect of crosslinking as well as presence of

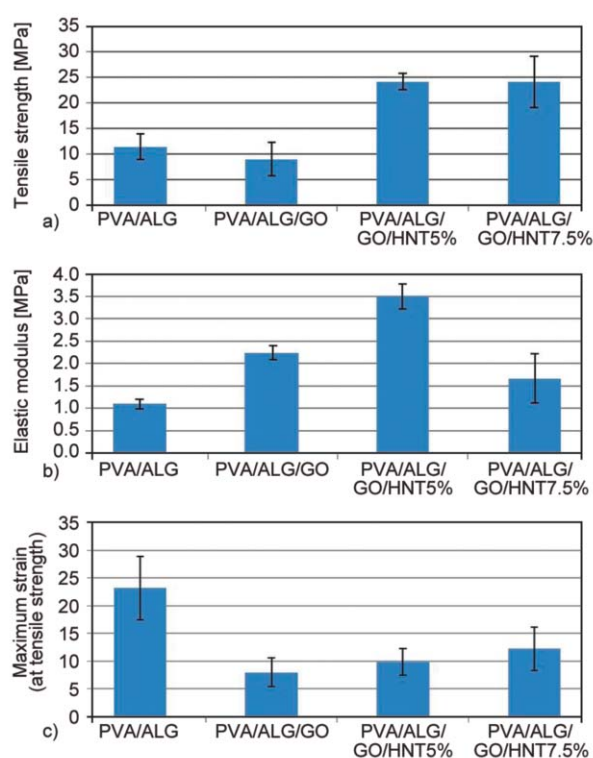


**Figure 5.** Tensile strength (a), elastic modulus (b), maximum strain (c) of uncrosslinked (PVA/ALG), cross-linked and HNT reinforced.

HNT nanotubes. However, the elastic modulus of PVA/ALG/GO/HNT7.5% nanofibers was lowered because the total concentration of polymer was significantly reduced due to the solution intercalation method used for the dispersion of HNT in polymer solutions.

The maximum strain for the samples is presented in Figure 5c. PVA/ALG nanofibers showed the highest strain significantly different with the crosslinked samples. The addition of crosslinkers reduces the strain of polymers as observed in this work.

### 3.5. Physicochemical stability and weight-swelling ratio

The long-term stability of microbial cell carriers is crucial factor for their re-usage in industrial application. Physicochemical studies on nanofibrous webs

in salt solutions for 30 days showed no breakage and physical damage for PVA/ALG/GO, PVA/ALG/GO/HNT5% and PVA/ALG/GO/HNT7.5%, while PVA/ALG web was completely disintegrated after 0.5 h in aqueous solutions. We therefore conclude that PVA/ALG/GO, PVA/ALG/GO/HNT5% and PVA/ALG/GO/HNT7.5% have acceptable mechanical resistance and chemical stability. Normal images of the electrospun PVA/ALG/GO/HNT5% and PVA/ALG/GO/HNT7.5% after this time are shown in Figure 6a.

The results of swelling ratio as a function of time for different prepared nanofibrous webs in distilled water are shown in Figure 6b. As the concentration of HNT increased from 0 to 7.5%, the rate of swelling increased from 308 to 450% after 4 h. Tham *et al.* [68] (2016) have reported that the presence of hydroxyl group in HNT causes to increase the water absorption.

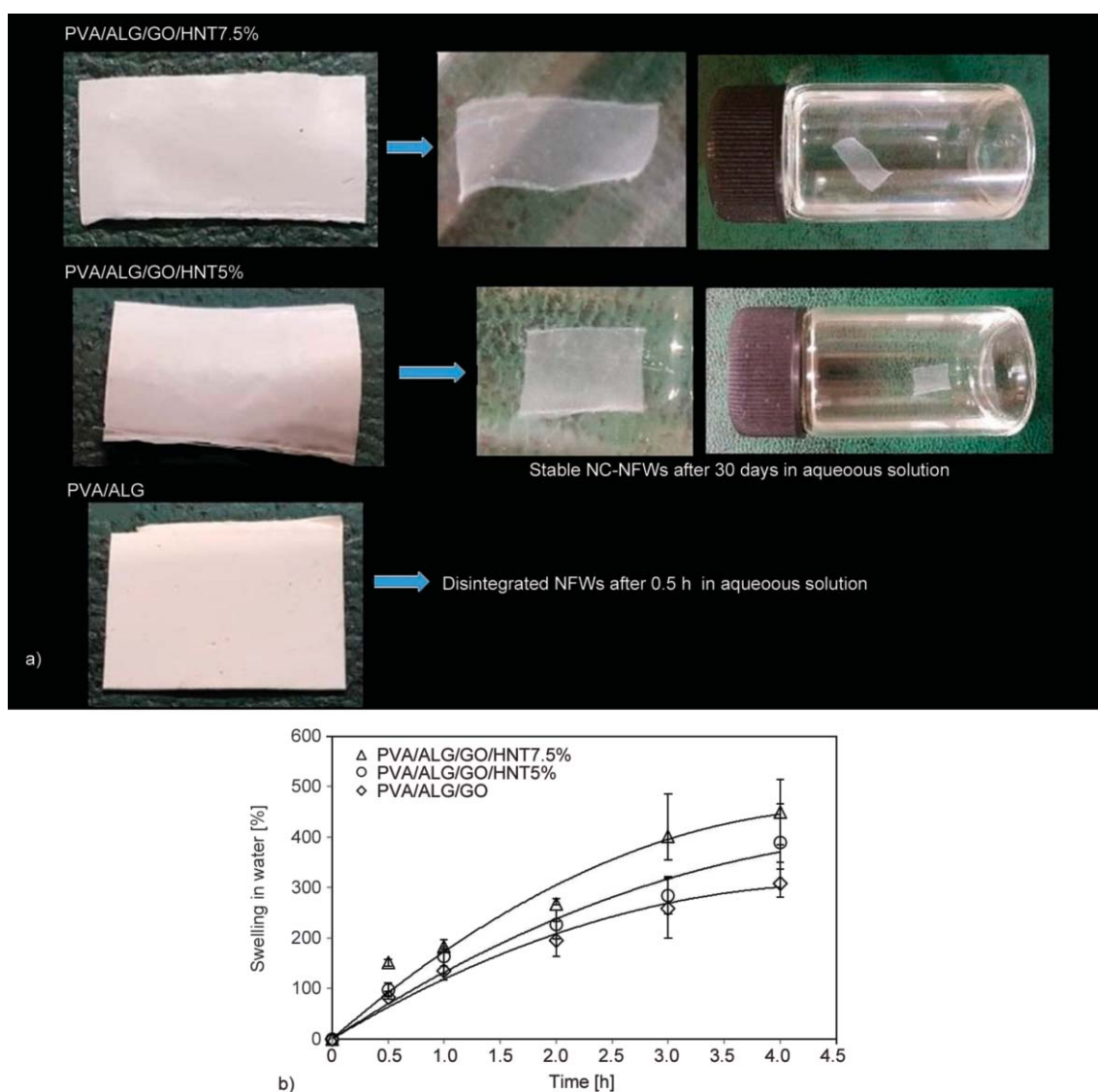


**Figure 6.** Normal images of NC-NFWs after experiments and storage time (a), weight-swelling ratio as a function of time for different prepared nanofiber webs (b).

Therefore, according to the results obtained from tensile strength, physicochemical stability and swelling ratio, PVA/ALG/GO/HNT5% and PVA/ALG/GO/HNT7.5% were selected for investigation of cell attachment and biodegradation study.

### 3.6. Microbial cell attachment

SEM images of the electrospun PVA/ALG/GO/HNT5% and PVA/ALG/GO/HNT7.5% after cell attachment are shown in Figure 7. Results show that the NC-NFWs were densely loaded with microbial cells. Comparison of the SEM images in Figure 7 for two nanocomposite webs shows that the concentration of cells which adhere to the PVA/ALG/GO/HNT7.5% mat was higher than the other one as a result of large specific surface area. Similarly, some previous researches have reported that an ideal carrier for microbial cell immobilization should have a large surface to volume ratio for cell adherence and growth [11, 25]. For determination of long-term stability, the recycled bacteria-immobilized nanofibrous webs were stored at 4 °C for 1 month in which webs were remained stable over this period of time. Additionally, detachment of immobilized cells was examined by three times washing of mats and its amount was also negligible. However, more research is needed to evaluate the bacterial detachment from the surfaces. Overall, the microbial cells attached on the surface of webs, are expected to be able to adequately utilize the substrates in the culture. Moreover, cell attachment to various biotic and abiotic surfaces can be facilitated by production of microbial exopolymers. Previous studies have reported that bacterial adhesion is reversible at first, but production of extracellular

polymeric substances can rapidly lead to an irreversible state and thereafter growth of a multi-layered bacterial biofilm [69, 70].

### 3.7. Time course of crude oil biodegradation

Biodegradability of heavy crude oil as sole carbon and energy source at concentration of 500 ppm was investigated in aqueous phase using different NC-NFWs and freely suspended cell system. Figure 8 illustrates the variation of culture optical density and removal percentage of heavy crude oil, showing an increase in  $OD_{600}$  and maximum growth is obtained by PVA/ALG/GO/HNT7.5%. A sharp increase occurs in optical density until the day 12 where it starts leveling off and finally it reaches 0.64. It is worth mention that no significant variation in  $OD_{600}$  value is found in the experiment for examination of microbial cell detachment throughout the experimental process. With regard to this result and also compatibility of hydrophilic nature of both microbial cell and matrix (ALG and PVA), it can be concluded that the attachment of microbial cells to surfaces mainly depends on hydrophobic interactions. However, additional investigation should be performed to confirm this result. Moreover, the obtained  $OD_{600}$  value in the experiment to investigate the possible matrix degradation was negligible compared to  $OD_{600}$  for bacteria-immobilized NC-NFWs that revealed no degradation of matrices in the experiments. At this condition, the maximum optical density of culture was found almost 0.1 after 24 h and remained consistent throughout the experimental process.

Similarly, the results of biodegradation after 14 days, show that improved crude oil removal was obtained

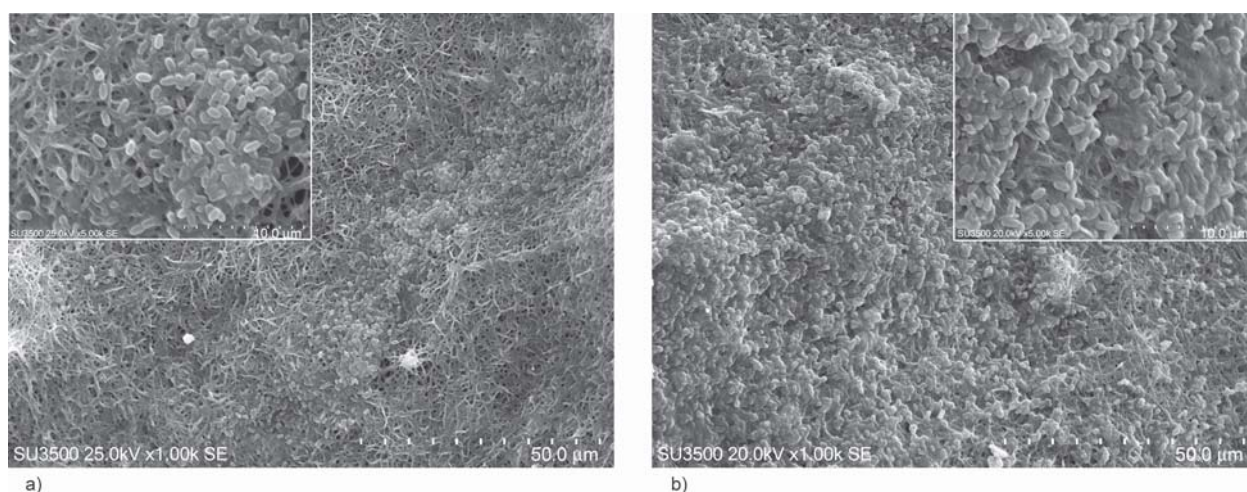


**Figure 7.** SEM images of the electrospun PVA/ALG/GO/HNT5% (a) and PVA/ALG/GO/HNT7.5% (b) after cell attachment at two different magnifications.



with immobilized cell compared to freely suspended cell systems due to the advantages of immobilization technique as we have previously discussed [15]. In the FC system, the total petroleum hydrocarbons (TPHs) removal was about 48%. For the control flasks containing empty NC-NFWs (matrices without bacterial cells), crude oil is degraded below 4% only at the end of the process. Similarly, Zahed *et al.* [71] (2010) have investigated biodegradation of light crude oil in contaminated seawater. According to their results, with initial crude oil concentrations of 100, 500, 1000 and 2000 ppm, removal of TPHs were 64.2, 55.7, 48.8 and 37.6%, respectively after 45 days.

The IC system with PVA/ALG/GO/HNT7.5% web showed a removal of about 85% of TPHs, whereas in the system with PVA/ALG/GO/HNT5%, the removal was of about 64%. To the best of our knowledge, no report exists in applying immobilization technique with cell attachment to a surface for biodegradation of heavy crude oil. Quek *et al.* [72] (1998) have reported that *Rhodococcus sp.* F92 immobilized in polyurethane foam (PUF) had shown maximum oil removal of about 80% in artificial seawater containing 0.5% (w/v) of Arabian light crude oil after 21 days. Zinjarde and Pant [73] (2000) have also reported that by immobilization of *Yarrowia lipolytica* in agar-alginate matrix, 92% removal of crude oil was observed at concentration of 1% (w/v) after 30 days. Obuekwe and Al-Muttawa [74] (2001) have observed that *Arthrobacter sp.* immobilized on styrofoam, sawdust and bran are able to degrade 37.5, 45 and 27.5% of crude oil at initial concentration of 800 ppm after 7 days, respectively. Therefore, it can be concluded that the presented NC-NFW shows the high performance of biodegradation and hence it can be a valuable matrix for enzyme and cell immobilization.

However, it is also worth mentioning that high surface area to weight ratio of NC-NFWs compared to traditional PVA/ALG beads and presence of HNT as an agent for enzyme immobilization are the main benefits of these prepared matrices. Similarly, Panchal *et al.* [75] (2018) have found that halloysite increases metabolism of oil-degrading bacteria without reducing growth rate. Jia *et al.* [76] (2003) have also reported that effective enzyme loading on polystyrene (PS) nanoparticles could be achieved up to 10 wt% due to a large surface area to weight ratio of the PS nanoparticles. We conclude that immobilization of produced enzymes during biodegradation process on HNT as well as microbial cells can facilitate pollutants removal. Furthermore, natural clay nanotubes such as HNT are abundantly available and biocompatible, therefore scale up of this technology for environmental remediation is feasible [77].

#### 4. Conclusions

To our knowledge, this work is the first research on reinforcing PVA/ALG nanofibrous web with HNT nanoclay. The present work shows that addition of HNT affects pore size and surface area to volume ratio as key criteria in selection of matrices for immobilization of biocatalysts such as microbial cells and enzymes. HNT improves matrix properties such as tensile strength and swelling ratio for usage in bioreactor or field scale. The other novelty of this work is the capability of modified PVA/ALG matrix to use for enzyme immobilization due to presence of HNT. Along with efficiently encapsulated bacteria, enzymes that produced during bacterial activity in the culture can be adsorbed and immobilized on HNT, which can facilitate the bio-chemical reactions and increase metabolism of pollutant-degrading bacteria. Also, this is the first report on heavy crude oil

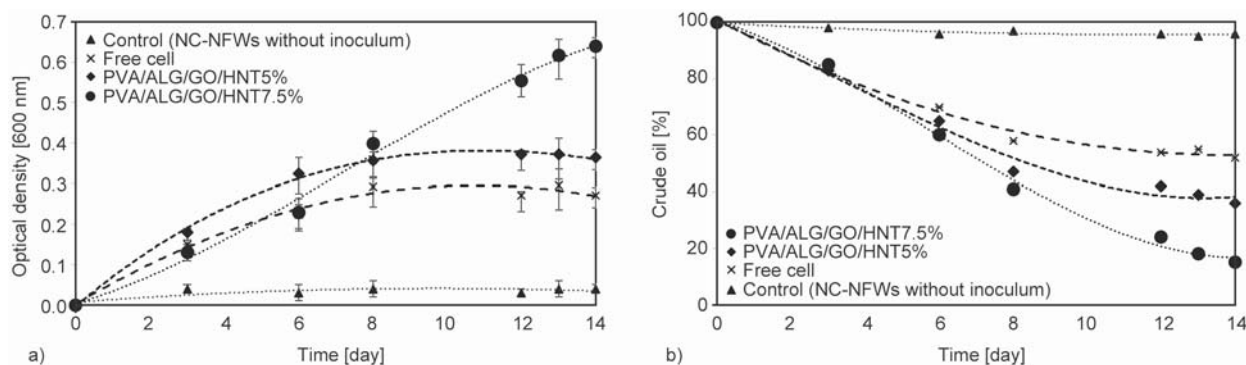


**Figure 8.** Time course of crude oil biodegradation using different NC-NFWs and free cell (a) culture optical density (b) removal percentage.

biodegradation in which the modified PVA/ALG/GO/ HNT webs were investigated at initial concentration of 500 ppm. The superiority of immobilized webs was attributed to the improved surface area, porosity of webs and the harmless physical method exploited compared to previous studies related to PVA/ALG matrices. Overall, these findings can have generic application for various biotechnological fields.

## Acknowledgements

This research was supported by Shahid Beheshti University, G.C. (grant number 600/253). The authors declare that there is no conflict of interests.

## References

- [1] Vidali M.: Bioremediation. An overview. *Pure and Applied Chemistry*, **73**, 1163–1172 (2001).  
<https://doi.org/10.1351/pac200173071163>
- [2] Singh A., Kuhad R. C., Ward O. P.: *Advances in applied bioremediation*. Springer, Berlin (2009).
- [3] Alvarez P. J. J., Illman W. A.: *Bioremediation and natural attenuation: Process fundamentals and mathematical models*. Wiley, Hoboken (2006).
- [4] Boopathy R.: Factors limiting bioremediation technologies. *Bioresource Technology*, **74**, 63–67 (2000).  
[https://doi.org/10.1016/S0960-8524\(99\)00144-3](https://doi.org/10.1016/S0960-8524(99)00144-3)
- [5] Karel S. F., Libicki S. B., Robertson C. R.: The immobilization of whole cells: Engineering principles. *Chemical Engineering Science*, **40**, 1321–1354 (1985).  
[https://doi.org/10.1016/0009-2509\(85\)80074-9](https://doi.org/10.1016/0009-2509(85)80074-9)
- [6] Willaert R. G., Baron G. V.: *Immobilized living cell systems: Modelling and experimental methods*. Wiley Chircester (1996).
- [7] Cunningham C. J., Ivshina I. B., Lozinsky V. I., Kuyukina M. S., Philp J. C.: Bioremediation of diesel-contaminated soil by microorganisms immobilised in polyvinyl alcohol. *International Biodeterioration and Biodegradation*, **54**, 167–174 (2004).  
<https://doi.org/10.1016/j.ibiod.2004.03.005>
- [8] Mancera-López M., Esparza-García F., Chávez-Gomez B., Rodríguez-Vázquez R., Saucedo-Castañeda G., Barrera-Cortés J.: Bioremediation of an aged hydrocarbon-contaminated soil by a combined system of biostimulation–bioaugmentation with filamentous fungi. *International Biodeterioration and Biodegradation*, **61**, 151–160 (2008).  
<https://doi.org/10.1016/j.ibiod.2007.05.012>
- [9] Mrozik A., Piotrowska-Seget Z.: Bioaugmentation as a strategy for cleaning up of soils contaminated with aromatic compounds. *Microbiological Research*, **165**, 363–375 (2010).  
<https://doi.org/10.1016/j.micres.2009.08.001>
- [10] Xu Y., Lu M.: Bioremediation of crude oil-contaminated soil: Comparison of different biostimulation and bioaugmentation treatments. *Journal of Hazardous Materials*, **183**, 395–401 (2010).  
<https://doi.org/10.1016/j.jhazmat.2010.07.038>
- [11] Cassidy M. B., Lee H., Trevors J. T.: Environmental applications of immobilized microbial cells: A review. *Journal of Industrial Microbiology*, **16**, 79–101 (1996).  
<https://doi.org/10.1007/BF01570068>
- [12] Partovinia A., Naeimpoor F.: Phenanthrene biodegradation by immobilized microbial consortium in polyvinyl alcohol cryogel beads. *International Biodeterioration and Biodegradation*, **85**, 337–344 (2013).  
<https://doi.org/10.1016/j.ibiod.2013.08.017>
- [13] Rosevear A., Kennedy J. F., Cabral J. M. S.: *Immobilized enzymes and cells*. Adam Hilger, Philadelphia (1987).
- [14] Shen Y., Yu T., Xie Y., Chen J., Ho S-H., Wang Y., Huang F.: Attached culture of *Chlamydomonas* sp. Jsc4 for biofilm production and TN/TP/Cu(II) removal. *Biochemical Engineering Journal*, **141**, 1–9 (2019).  
<https://doi.org/10.1016/j.bej.2018.09.017>
- [15] Partovinia A., Rasekh B.: Review of the immobilized microbial cell systems for bioremediation of petroleum hydrocarbons polluted environments. *Critical Reviews in Environmental Science and Technology*, **48**, 1–38 (2018).  
<https://doi.org/10.1080/10643389.2018.1439652>
- [16] Krasowska A., Sigler K.: How microorganisms use hydrophobicity and what does this mean for human needs? *Frontiers in Cellular and Infection Microbiology*, **4**, 112/1–112/7 (2014).  
<https://doi.org/10.3389/fcimb.2014.00112>
- [17] Wang Z., Chen Z., Yang L., Tan F., Wang Y., Li Q., Chang Y-I., Zhong C-J., He N.: Effect of surface physicochemical properties on the flocculation behavior of *Bacillus licheniformis*. *RSC Advances*, **7**, 16049–16056 (2017).  
<https://doi.org/10.1039/C6RA28057A>
- [18] Eş I., Vieira J. D. G., Amaral A. C.: Principles, techniques, and applications of biocatalyst immobilization for industrial application. *Applied Microbiology and Biotechnology*, **99**, 2065–2082 (2015).  
<https://doi.org/10.1007/s00253-015-6390-y>
- [19] Buitelaar R. M., Bucke C., Tramper J., Wijffels R. H.: *Immobilized cells: Basics and applications*. Elsevier, Amsterdam (1996).
- [20] Cortez S., Nicolau A., Flickinger M. C., Mota M.: Bio-coatings: A new challenge for environmental biotechnology. *Biochemical Engineering Journal*, **121**, 25–37 (2017).  
<https://doi.org/10.1016/j.bej.2017.01.004>
- [21] Siripattanakul S., Khan E.: Fundamentals and applications of entrapped cell bioaugmentation for contaminant removal. in ‘Emerging environmental technologies’ (ed.: Shah V.) Springer, Dordrecht, 147–169 (2010).  
[https://doi.org/10.1007/978-90-481-3352-9\\_7](https://doi.org/10.1007/978-90-481-3352-9_7)

- [22] Wang X., Gong Z. Q., Li P. J., Zhang L. H.: Degradation of pyrene in soils by free and immobilized yeasts, candida tropicals. Bulletin of Environmental Contamination and Toxicology, **78**, 522–526 (2007).  
<https://doi.org/10.1007/s00128-007-9156-0>
- [23] Idris A., Zain N. A. M., Suhaimi M. S.: Immobilization of Baker's yeast invertase in PVA–alginate matrix using innovative immobilization technique. Process Biochemistry, **43**, 331–338 (2008).  
<https://doi.org/10.1016/j.procbio.2007.12.008>
- [24] Zain N. A. M., Suhaimi M. S., Idris A.: Development and modification of PVA–alginate as a suitable immobilization matrix. Process Biochemistry, **46**, 2122–2129 (2011).  
<https://doi.org/10.1016/j.procbio.2011.08.010>
- [25] Liang Y., Zhang X., Dai D., Li G.: Porous biocarrier-enhanced biodegradation of crude oil contaminated soil. International Biodeterioration and Biodegradation, **63**, 80–87 (2009).  
<https://doi.org/10.1016/j.ibiod.2008.07.005>
- [26] Salalha W., Kuhn J., Dror Y., Zussman E.: Encapsulation of bacteria and viruses in electrospun nanofibres. Nanotechnology, **17**, 4675–4681 (2006).  
<https://doi.org/10.1088/0957-4484/17/18/025>
- [27] San Keskin N. O., Celebioglu A., Sarioglu O. F., Ozkan A. D., Uyar T., Tekinay T.: Removal of a reactive dye and hexavalent chromium by a reusable bacteria attached electrospun nanofibrous web. RSC Advances, **5**, 86867–86874 (2015).  
<https://doi.org/10.1039/C5RA15601G>
- [28] San Keskin N. O., Celebioglu A., Sarioglu O. F., Uyar T., Tekinay T.: Encapsulation of living bacteria in electrospun cyclodextrin ultrathin fibers for bioremediation of heavy metals and reactive dye from wastewater. Colloids and Surfaces B: Biointerfaces, **161**, 169–176 (2018).  
<https://doi.org/10.1016/j.colsurfb.2017.10.047>
- [29] Sarioglu O. F., Celebioglu A., Tekinay T., Uyar T.: Bacteria-immobilized electrospun fibrous polymeric webs for hexavalent chromium remediation in water. International Journal of Environmental Science and Technology, **13**, 2057–2066 (2016).  
<https://doi.org/10.1007/s13762-016-1033-0>
- [30] Sarioglu O. F., Keskin N. O. S., Celebioglu A., Tekinay T., Uyar T.: Bacteria encapsulated electrospun nanofibrous webs for remediation of methylene blue dye in water. Colloids and Surfaces B: Biointerfaces, **152**, 245–251 (2017).  
<https://doi.org/10.1016/j.colsurfb.2017.01.034>
- [31] Klein S., Kuhn J., Avrahami R., Tarre S., Belavski M., Green M., Zussman E.: Encapsulation of bacterial cells in electrospun microtubes. Biomacromolecules, **10**, 1751–1756 (2009).  
<https://doi.org/10.1021/bm900168v>
- [32] Eroglu E., Agarwal V., Bradshaw M., Chen X., Smith S. M., Raston C. L., Swaminathan Iyer K.: Nitrate removal from liquid effluents using microalgae immobilized on chitosan nanofiber mats. Green Chemistry, **14**, 2682–2685 (2012).  
<https://doi.org/10.1039/C2GC35970G>
- [33] Sarma S. J., Pakshirajan K.: Surfactant aided biodegradation of pyrene using immobilized cells of *Mycobacterium frederiksbergense*. International Biodeterioration and Biodegradation, **65**, 73–77 (2011).  
<https://doi.org/10.1016/j.ibiod.2010.09.004>
- [34] Ferreira L., Rosales E., Sanromán M. A., Pazos M.: Preliminary testing and design of permeable bioreactive barrier for phenanthrene degradation by *Pseudomonas stutzeri* CECT 930 immobilized in hydrogel matrices. Journal of Chemical Technology and Biotechnology, **90**, 500–506 (2014).  
<https://doi.org/10.1002/jctb.4338>
- [35] Ramteke L. P., Gogate P. R.: Removal of benzene, toluene and xylene (BTX) from wastewater using immobilized modified prepared activated sludge (MPAS). Journal of Chemical Technology and Biotechnology, **91**, 456–466 (2014).  
<https://doi.org/10.1002/jctb.4599>
- [36] Lin C., Gan L., Chen Z., Megharaj M., Naidu R.: Biodegradation of naphthalene using a functional biomaterial based on immobilized *Bacillus fusiformis* (BFN). Biochemical Engineering Journal, **90**, 1–7 (2014).  
<https://doi.org/10.1016/j.bej.2014.05.003>
- [37] Nunes M. A. P., Vila-Real H., Fernandes P. C. B., Ribeiro M. H. L.: Immobilization of naringinase in PVA–alginate matrix using an innovative technique. Applied Biochemistry and Biotechnology, **160**, 2129–2147 (2010).  
<https://doi.org/10.1007/s12010-009-8733-6>
- [38] Zhang Y., Zhu P. C., Edgren D.: Crosslinking reaction of poly(vinyl alcohol) with glyoxal. Journal of Polymer Research, **17**, 725–730 (2010).  
<https://doi.org/10.1007/s10965-009-9362-z>
- [39] Tully J., Yendluri R., Lvov Y.: Halloysite clay nanotubes for enzyme immobilization. Biomacromolecules, **17**, 615–621 (2016).  
<https://doi.org/10.1021/acs.biomac.5b01542>
- [40] Price R. R., Gaber B. P., Lvov Y.: *In-vitro* release characteristics of tetracycline HCl, khellin and nicotinamide adenine dinucleotide from halloysite; A cylindrical mineral. Journal of Microencapsulation, **18**, 713–722 (2001).  
<https://doi.org/10.1080/02652040010019532>
- [41] Veerabadran N. G., Price R. R., Lvov Y. M.: Clay nanotubes for encapsulation and sustained release of drugs. Nano, **02**, 115–120 (2007).  
<https://doi.org/10.1142/s1793292007000441>



- [42] Chao C., Liu J., Wang J., Zhang Y., Zhang B., Zhang Y., Xiang X., Chen R.: Surface modification of halloysite nanotubes with dopamine for enzyme immobilization. *ACS Applied Materials and Interfaces*, **5**, 10559–10564 (2013).  
<https://doi.org/10.1021/am4022973>
- [43] Oh Y-S., Maeng J., Kim S-J.: Use of microorganism-immobilized polyurethane foams to absorb and degrade oil on water surface. *Applied Microbiology and Biotechnology*, **54**, 418–423 (2000).  
<https://doi.org/10.1007/s002530000384>
- [44] Siripattanakul S., Wirojanagud W., McEvoy J., Khan E.: Effect of cell-to-matrix ratio in polyvinyl alcohol immobilized pure and mixed cultures on atrazine degradation. *Water, Air, and Soil Pollution: Focus*, **8**, 257–266 (2008).  
<https://doi.org/10.1007/s11267-007-9158-2>
- [45] Gentili A. R., Cubitto M. A., Ferrero M., Rodríguez M. S.: Bioremediation of crude oil polluted seawater by a hydrocarbon-degrading bacterial strain immobilized on chitin and chitosan flakes. *International Biodeterioration and Biodegradation*, **57**, 222–228 (2006).  
<https://doi.org/10.1016/j.ibiod.2006.02.009>
- [46] Islam M. S., Karim M. R.: Fabrication and characterization of poly(vinyl alcohol)/alginate blend nanofibers by electrospinning method. *Colloids and Surfaces A: Physicochemical and Engineering Aspects*, **366**, 135–140 (2010).  
<https://doi.org/10.1016/j.colsurfa.2010.05.038>
- [47] Seeram R., Teik-cheng L., Kazutoshi F.: An introduction to electrospinning and nanofibers. World Scientific Publishing, Singapore (2005).
- [48] Koosha M., Mirzadeh H., Shokrgozar M. A., Farokhi M.: Nanoclay-reinforced electrospun chitosan/PVA nanocomposite nanofibers for biomedical applications. *RSC Advances*, **5**, 10479–10487 (2015).  
<https://doi.org/10.1039/C4RA13972K>
- [49] Marras S. I., Kladi K. P., Tsivintzelis I., Zuburtikudis I., Panayiotou C.: Biodegradable polymer nanocomposites: The role of nanoclays on the thermomechanical characteristics and the electrospun fibrous structure. *Acta Biomaterialia*, **4**, 756–765 (2008).  
<https://doi.org/10.1016/j.actbio.2007.12.005>
- [50] Wang M., Hsieh A. J., Rutledge G. C.: Electrospinning of poly(MMA-co-MAA) copolymers and their layered silicate nanocomposites for improved thermal properties. *Polymer*, **46**, 3407–3418 (2005).  
<https://doi.org/10.1016/j.polymer.2005.02.099>
- [51] Hong J. H., Jeong E. H., Lee H. S., Baik D. H., Seo S. W., Youk J. H.: Electrospinning of polyurethane/organically modified montmorillonite nanocomposites. *Journal of Polymer Science Part B: Polymer Physics*, **43**, 3171–3177 (2005).  
<https://doi.org/10.1002/polb.20610>
- [52] Li H., Li P., Hua T., Zhang Y., Xiong X., Gong Z.: Bio-remediation of contaminated surface water by immobilized *Micrococcus roseus*. *Environmental Technology*, **26**, 931–940 (2005).  
<https://doi.org/10.1080/09593332608618504>
- [53] Moslemy P., Guiot S. R., Neufeld R. J.: Encapsulation of bacteria for biodegradation of gasoline hydrocarbons. in ‘Immobilization of enzymes and cells’ (ed.: Guisán J.) Springer, Berlin, 415–426 (2006).  
[https://doi.org/10.1007/978-1-59745-053-9\\_36](https://doi.org/10.1007/978-1-59745-053-9_36)
- [54] Koosha M., Mirzadeh H.: Electrospinning, mechanical properties, and cell behavior study of chitosan/PVA nanofibers. *Journal of Biomedical Materials Research Part A*, **103**, 3081–3093 (2015).  
<https://doi.org/10.1002/jbm.a.35443>
- [55] Abdel Aziz M. S., Salama H. E., Sabaa M. W.: Bio-based alginate/castor oil edible films for active food packaging. *LWT*, **96**, 455–460 (2018).  
<https://doi.org/10.1016/j.lwt.2018.05.049>
- [56] Huang D., Wang W., Kang Y., Wang A.: A chitosan/poly(vinyl alcohol) nanocomposite film reinforced with natural halloysite nanotubes. *Polymer Composites*, **33**, 1693–1699 (2012).  
<https://doi.org/10.1002/pc.22302>
- [57] Shalumon K. T., Anulekha K. H., Nair S. V., Nair S. V., Chennazhi K. P., Jayakumar R.: Sodium alginate/poly(vinyl alcohol)/nano ZnO composite nanofibers for antibacterial wound dressings. *International Journal of Biological Macromolecules*, **49**, 247–254 (2011).  
<https://doi.org/10.1016/j.ijbiomac.2011.04.005>
- [58] Lawrie G., Keen I., Drew B., Chandler-Temple A., Rintoul L., Fredericks P., Grøndahl L.: Interactions between alginate and chitosan biopolymers characterized using FTIR and XPS. *Biomacromolecules*, **8**, 2533–2541 (2007).  
<https://doi.org/10.1021/bm070014y>
- [59] Sakugawa K., Ikeda A., Takemura A., Ono H.: Simplified method for estimation of composition of alginates by FTIR. *Journal of Applied Polymer Science*, **93**, 1372–1377 (2004).  
<https://doi.org/10.1002/app.20589>
- [60] Engdahl A., Nelander B.: Infrared spectrum of cis-glyoxal. *Chemical Physics Letters*, **148**, 264–268 (1988).  
[https://doi.org/10.1016/0009-2614\(88\)80312-9](https://doi.org/10.1016/0009-2614(88)80312-9)
- [61] Afshar H. A., Ghaee A.: Preparation of aminated chitosan/alginate scaffold containing halloysite nanotubes with improved cell attachment. *Carbohydrate Polymers*, **151**, 1120–1131 (2016).  
<https://doi.org/10.1016/j.carbpol.2016.06.063>
- [62] Bordepong S., Bhongsuwan D., Punggrassami T., Bhongsuwan T.: Characterization of halloysite from Thung Yai district, Nakhon Si Thammarat Province, in Southern Thailand. *Songklanakarin Journal of Science and Technology*, **33**, 599–607 (2011).

- [63] Zhou W. Y., Guo B., Liu M., Liao R., Rabie A. B. M., Jia D.: Poly(vinyl alcohol)/halloysite nanotubes bio-nanocomposite films: Properties and *in vitro* osteoblasts and fibroblasts response. *Journal of Biomedical Materials Research Part A*, **93A**, 1574–1587 (2009).  
<https://doi.org/10.1002/jbm.a.32656>
- [64] Zeng X., Sun Z., Wang H., Wang Q., Yang Y.: Supramolecular gel composites reinforced by using halloysite nanotubes loading with *in-situ* formed Fe<sub>3</sub>O<sub>4</sub> nanoparticles and used for dye adsorption. *Composites Science and Technology*, **122**, 149–154 (2016).  
<https://doi.org/10.1016/j.compscitech.2015.11.025>
- [65] Liu M., Guo B., Du M., Jia D.: Drying induced aggregation of halloysite nanotubes in polyvinyl alcohol/halloysite nanotubes solution and its effect on properties of composite film. *Applied Physics A*, **88**, 391–395 (2007).  
<https://doi.org/10.1007/s00339-007-3995-8>
- [66] Swapna V. P., Selvin Thomas P., Suresh K. I., Saranya V., Rahana M. P., Ranimol S.: Thermal properties of poly (vinyl alcohol)(PVA)/halloysite nanotubes reinforced nanocomposites. *International Journal of Plastics Technology*, **19**, 124–136 (2015).  
<https://doi.org/10.1007/s12588-015-9106-3>
- [67] Fujii K., Nakagaito A. N., Takagi H., Yonekura D.: Sulfuric acid treatment of halloysite nanoclay to improve the mechanical properties of PVA/halloysite transparent composite films. *Composite Interfaces*, **21**, 319–327 (2014).  
<https://doi.org/10.1080/15685543.2014.876307>
- [68] Tham W. L., Poh B. T., Ishak Z. A. M., Chow W. S.: Characterisation of water absorption of biodegradable poly(lactic acid)/halloysite nanotube nanocomposites at different temperatures. *Journal of Engineering Science*, **12**, 13–25 (2016).
- [69] Gusnaniar N., van der Mei H., Qu W., Nuryastuti T., Hooymans J. M. M., Sjollem J., Busscher H.: Physico-chemistry of bacterial transmission versus adhesion. *Advances in Colloid and Interface Science*, **250**, 15–24 (2017).  
<https://doi.org/10.1016/j.cis.2017.11.002>
- [70] Hou J., Veeregowda D. H., van de Belt-Gritter B., Busscher H., van der Mei H.: Extracellular polymeric matrix production and relaxation under fluid shear and mechanical pressure in *Staphylococcus aureus* biofilms. *Applied and Environmental Microbiology*, **84**, e01516–17/1-e01516-17/14 (2018).  
<https://doi.org/10.1128/AEM.01516-17>
- [71] Zahed M. A., Aziz H. A., Isa M. H., Mohajeri L.: Effect of initial oil concentration and dispersant on crude oil biodegradation in contaminated seawater. *Bulletin of Environmental Contamination and Toxicology*, **84**, 438–442 (2010).  
<https://doi.org/10.1007/s00128-010-9954-7>
- [72] Quek E., Ting Y-P., Tan H. M.: *Rhodococcus* sp. F92 immobilized on polyurethane foam shows ability to degrade various petroleum products. *Bioresource Technology*, **97**, 32–38 (2006).  
<https://doi.org/10.1016/j.biortech.2005.02.031>
- [73] Zinjarde S. S., Pant A.: Crude oil degradation by free and immobilized cells of *Yarrowia lipolytica* NCIM 3589. *Journal of Environmental Science and Health, Part A*, **35**, 755–763 (2000).  
<https://doi.org/10.1080/10934520009377000>
- [74] Obuekwe C. O., Al-Muttawa E. M.: Self-immobilized bacterial cultures with potential for application as ready-to-use seeds for petroleum bioremediation. *Biotechnology Letters*, **23**, 1025–1032 (2001).  
<https://doi.org/10.1023/a:1010544320118>
- [75] Panchal A., Swientoniewski L. T., Omarova M., Yu T., Zhang D., Blake D. A., John V., Lvov Y. M.: Bacterial proliferation on clay nanotube pickering emulsions for oil spill bioremediation. *Colloids and Surfaces B: Biointerfaces*, **164**, 27–33 (2018).  
<https://doi.org/10.1016/j.colsurfb.2018.01.021>
- [76] Jia H., Zhu G., Wang P.: Catalytic behaviors of enzymes attached to nanoparticles: The effect of particle mobility. *Biotechnology and Bioengineering*, **84**, 406–414 (2003).  
<https://doi.org/10.1002/bit.10781>
- [77] Zhang Y., Tang A., Yang H., Ouyang J.: Applications and interfaces of halloysite nanocomposites. *Applied Clay Science*, **119**, 8–17 (2016).  
<https://doi.org/10.1016/j.clay.2015.06.034>